

## Computational study of electronic, spectroscopic and chemical properties of Cu<sub>n</sub> (n=2-8) nanoclusters for CO adsorption

Razieh Habibpour<sup>1\*</sup>; Eslam Kashi<sup>1</sup>; Raheleh Vaziri<sup>2</sup>

<sup>1</sup>Department of Chemical Technologies, Iranian Research Organization for Science and Technology, Tehran, Iran

<sup>2</sup>Department of Chemistry, Payame Noor University, Tehran, Iran

Received 10 December 2016; revised 04 March 2017; accepted 03 April 2017; available online 05 April 2017

### Abstract

First-principle calculations were carried out to investigate the adsorption of CO over Cu<sub>n</sub> nanoclusters. The structural, spectroscopic and electronic properties like optimized geometries, HOMO (highest occupied molecular orbital) and LUMO (lowest unoccupied molecular orbital) energy levels, binding energy, adsorption energy, vibrational frequency and density of states (DOSs) of the pure Cu<sub>n</sub> nanoclusters, and Cu<sub>n</sub>CO complexes in their ground state were thoroughly analyzed. The CO adsorbed on the Cu<sub>n</sub> nanoclusters showed a stretch frequency at 1950-2052 cm<sup>-1</sup>, which was red-shifted relative to that of gas-phase CO (2143 cm<sup>-1</sup>). This red-shift was believed to arise from the charge transfer from the Cu metal d states to the CO antibonding 2π\* level. The CO adsorption on the Cu nanoclusters was chemisorption in nature with the Cu-C bond length (adsorption height) in the range of 1.85-1.92 Å.

**Keywords:** B3LYP; CO adsorption; Cu nanoclusters; DOS; LanL2DZ.

### How to cite this article

Habibpour R., Kashi E., Vaziri R., Computational study of electronic, spectroscopic and chemical properties of Cu<sub>n</sub>(n=2-8) nanoclusters for CO adsorption. *Int. J. Nano Dimens.*, 2017; 8(2): 114-123., DOI: [10.22034/ijnd.2017.24951](https://doi.org/10.22034/ijnd.2017.24951)

## INTRODUCTION

Nanoclusters are of great scientific interest in fundamental science and industrial applications as they are, in effect, a bridge between bulk materials and atomic or molecular structures [1-3]. They have size-dependent properties such as tailoring of optical gap, unusual magnetism, and enhanced catalytic activity. However, a bulk material should have constant physical properties regardless of its size [4, 5]. The nanoclusters of Cu and other transitional metals have attracted the attention of not only chemists and physicists but also biologists, computer scientists, electronic engineers, and metallurgists. They have potential applications in microelectronics, photovoltaics, imaging and display technologies, sensing devices, thin film coating, molecular electronics, and catalysis [6, 7].

Copper has been identified as an important catalytic agent for carbon monoxide, CO, and oxidation [8]. Metal clusters have been proposed

as molecular model systems for the chemisorption on extended metal surfaces. The similarity between a metal surface and small metal clusters that typically only contain between 2 and 10 atoms has been theoretically useful to gain insight into interactions between a metal center and organic or inorganic reactants [9]. The CO molecule is one of the most widely studied ligands in metal cluster chemistry as well as metal surface science. CO is a very suitable probe molecule to characterize the different binding sites on catalytic surfaces [10, 11]. The CO adsorption on several Cu systems has been studied by numerous groups using different surface science techniques [12-14]. The mechanism of CO binding to transition metals (TM) is well understood. According to the Blyholder model [15], it can be described in terms of an σ-donation of an electron from CO to the metal and p-back donation from the metal to CO. It is known that the catalytic activity of the catalyst can be greatly dependent on the particle size and

\* Corresponding Author Email: [habibpour@irost.ir](mailto:habibpour@irost.ir)

its surface chemistry [16].

In this report, the interaction between CO and  $\text{Cu}_n$  ( $n=2-8$ ) nanoclusters is investigated by means of the density functional theory (DFT). We present a detailed investigation of the geometry, binding energy, vibrational frequency, density of states, and HOMO-LUMO energies for  $\text{Cu}_n$  nanoclusters. Additionally, reactivity descriptors such as electronegativity, chemical hardness, and softness index of the lowest-energy isomers of these nanoclusters are estimated to study their relative stabilities.

## EXPERIMENTAL

### Computational Details

The calculations were performed using the density functional (DFT) theory under generalized gradient approximation. The B3LYP [17] exchange-correlation hybrid functional was selected and appeared to give reliable results for the considered systems. Since full electron computation was more time consuming, it was appropriate to present effective core potentials while taking into account some relativistic effects for the Cu atoms in order to describe the inner core electrons. For this reason, the Lan12DZ [18] basis set was chosen as it deals clearly with valence electrons through a split valence polarized basis set, retaining 19 electrons per Cu atom ( $3s^23p^63d^{10}4s^1$ ). Carbon and oxygen were treated with the 6-311G basis set. The calculated bond length and bond energy for CO were  $1.127 \text{ \AA}$  and  $11.02 \text{ eV}$ , respectively, which was in good agreement with experimental values of  $1.128 \text{ \AA}$  and  $11.24 \text{ eV}$  [19]. The interaction of the CO molecule with Cu nanoclusters was fully optimized without symmetry restrictions in different adsorption sites and orientations on the Cu nanoclusters. All the calculations were performed using the Gaussian 09 program [20].

## RESULTS AND DISCUSSION

### Geometries of $\text{Cu}_n$ ( $n=2-8$ ) nanoclusters

Initially, the structures of the  $\text{Cu}_n$  ( $n=2-8$ ) nanoclusters were generated and optimized by careful consideration of the previously reported stable geometries [21,22]. Then, the structural properties of the neutral  $\text{Cu}_n$  ( $n=2-8$ ) nanoclusters were restudied before studying the interaction of  $\text{Cu}_n$  nanoclusters with CO. All of these initial structures were completely optimized by relaxing the atomic positions by minimizing the total energy until the force acting on each atom became

negligible. In Table 1, the calculated electronic and spectroscopic parameters of the smallest  $\text{Cu}_n$  nanoclusters ( $\text{Cu}_2$ ) were compared with former experimental data [23, 24]. The results showed suitable agreement with the experimental values.

According to the results (as shown in Fig. 1), the clusters with  $n=4-6$  preferred 2 dimensional (2D) planar structures while larger clusters ( $n=7, 8$ ) stabilized in 3D geometries. Since the valence charge density of 2D structures was distributed among the lower number of bonds, the 2D structures had lower average coordination and shorter average bond length when compared with the 3D structures that had more bonds. Therefore, each of the bonds in the 2D isomers was stronger and shorter with respect to 3D isomers. The stability trend of  $\text{Cu}_n$  nanoclusters reflected the competition between the individual bond strength and the total number of bonds. It was observed that in the smaller sizes, the stronger individual bonds led to stability while the average coordination overcame and stabilized the 3D structures in the larger structures. After the accurate atomic relaxation of the relevant configurations and comparison of their minimized total energies, the most stable isomers of the pure  $\text{Cu}_n$  nanoclusters were identified and used for the CO adsorption study.

A generally valid linear correlation relationship existed as follows: between the calculated HOMO energies and the experimental/calculated ionization potentials; between the calculated LUMO energies and experimental/calculated electron affinities; between the calculated average HOMO/LUMO energies and electronegativity values; and between the calculated HOMO-LUMO energy gaps and hardness/softness values. Consequently, the calculated HOMO and LUMO energies can be used to semi-quantitatively estimate the IPs, EAs,  $\chi$ ,  $\eta$  and  $\sigma$  [25]. These quantum chemical parameters were measured using Equations 1-3 and their values are listed in Table 2.

$$\text{IP} = -E_{\text{HOMO}} \quad \text{EA} = -E_{\text{LUMO}} \quad (1)$$

Assuming that these relations are valid within the DFT frame, the electronegativity ( $\chi$ ) and hardness ( $\eta$ ) can be estimated with:

$$\chi = \left( \frac{\text{IP} + \text{EA}}{2} \right) \quad \eta = \left( \frac{\text{IP} - \text{EA}}{2} \right) \quad (2)$$

Softness is given by

$$\sigma = 1/\eta \quad (3)$$

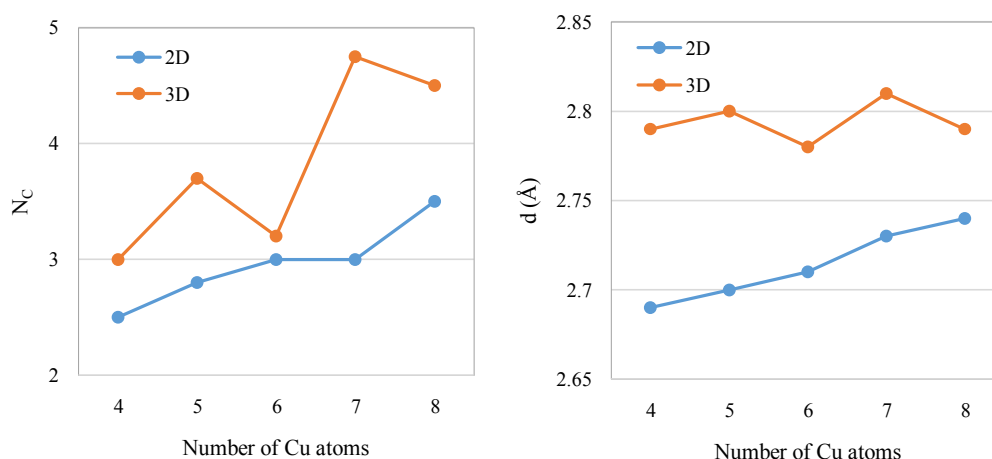


Fig. 1: Coordination number (NC) of Cu atoms and average bond length ( $d$  in Å) in the most stable 2D and 3D isomers of  $Cu_n$  ( $n=2-8$ ) nanoclusters.

Table 1: Comparison of calculated and experimental values of the bond length (R), Ionization Potential (IP) and vibrational frequencies (Frec.) of  $Cu_2$  cluster.

	Cal.	Exp.
R (Å)	2.25	2.22 [21]
IP (ev)	5.59	7.90 [22]
Frec.	256.02	265 [21]

Table 2: HOMO-LUMO energy gap, ionization potential, electron affinity, electronegativity, hardness, and softness of  $Cu_n$  nanoclusters.

	$\Delta E_{\text{HOMO-LUMO}}$	IP	EA	$\chi$	$\eta$	$\sigma$
$Cu_2$	3.254	5.5892	2.3347	3.9619	1.6272	0.6145
$Cu_3$	1.393	4.0517	2.6558	3.3551	0.6966	1.4355
$Cu_4$	1.904	4.7538	2.8364	3.7987	0.9523	1.0500
$Cu_5$	1.338	4.5524	3.2136	3.8830	0.6694	1.4938
$Cu_6$	3.878	4.8322	0.9536	2.8929	1.9393	0.5156
$Cu_7$	1.724	4.272	2.548	3.4123	0.8624	1.1601
$Cu_8$	1.925	5.0811	3.156	4.1185	0.9625	1.0389

According to Table 2, one can note that the clusters with an even number of atoms had a greater HOMO-LUMO gap, and therefore were expected to be less reactive than clusters with an odd number of atoms. The stability displayed by the even-number electron clusters was due to their closed-shell configuration that always produced additional stability.

#### CO adsorption on $Cu_n$ ( $n=2-8$ ) nanoclusters

The most stable structures of  $Cu_n$  CO complexes are displayed in Table 3. Once the optimization of

cluster geometry was executed, the vibrational frequencies as the second derivative of the energy with respect to the nuclear positions were calculated. It is worth noting that the interaction of the CO molecule with each cluster only moderately modified the cluster geometry. Full geometry optimization was accomplished for  $Cu_n$  CO complexes, yielding the binding energy, adsorption energy, the adsorption height ( $h$ ), and the C-O bond length (Table 3). The CO binding energy (BE) per atom is defined by the following equation:

$$BE = [E(Cu_nCO) - nE(Cu) - E(C) - E(O)] / (n+2) \quad (4)$$

The adsorption energy was calculated according to the following equation:

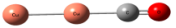
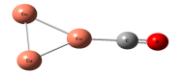
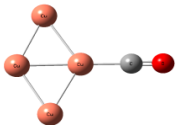
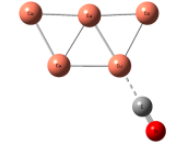
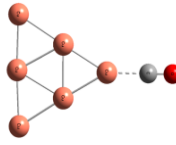
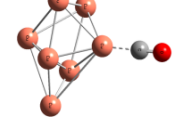
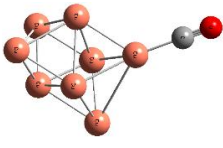
$$E_{ads} = E(Cu_nCO) - E(CO) - E(Cu_n) \quad (5)$$

where  $E(Cu_nCO)$ ,  $E(Cu_n)$ ,  $E(CO)$ ,  $E(Cu)$ ,  $E(C)$  and  $E(O)$  are the energy of the  $Cu_nCO$  complex,  $Cu_n$

nanocluster, CO molecule, Cu, C, and O atoms, respectively.

The dipole moment in a molecule is principally used to study the intermolecular interactions because the higher the dipole moment, the stronger the intermolecular interactions will be. For these  $Cu_nCO$  complexes,  $Cu_6CO$  had the highest dipole moment (2.82 D) (Table 3).

Table 3. Optimized structure, binding energy (eV), adsorption energy (eV), adsorption height (h) (Å), C-O bond length (Å), and dipole moment (Debye) of  $Cu_nCO$  complexes.

Optimized structure	binding energy (eV)	adsorption energy (Kcal/mol)	adsorption height (h or Cu-C distance) (Å)	C-O bond length (Å)	dipole moment (Debye)	Energy (Hartree) Before adsorption	Energy (Hartree) After adsorption
	93.33	19.1	1.88	1.13	1.83	-392.72	-505.62
	81.63	27.7	1.85	1.14	0.90	-588.53	-701.79
	77.55	27.9	1.85	1.14	0.44	-785.12	-897.99
	71.56	17.5	1.91	1.14	0.62	-981.24	-1094.16
	69.93	13.2	1.92	1.13	2.82	-1177.63	-1290.36
	67.21	13.0	1.92	1.13	1.23	-1373.49	-1486.56
	67.21	16.2	1.92	1.13	1.96	-1570.28	-1682.75

On the other hand, this complex had the lowest adsorption and binding energy and the highest HOMO-LUMO gap.

The energy comparison of  $Cu_n$  nanoclusters and  $Cu_nCO$  complexes indicated that CO adsorption led to greater stability (Fig. 2). It can be explained by the charge transfer from the  $Cu_n$  nanoclusters to the CO molecule, which enhanced the electrostatic interaction in the Cu–C bonding.

In Table 4, the calculated vibrational frequencies of the  $Cu_n$  nanoclusters and  $Cu_nCO$  complexes are presented. The more probable frequencies for each system are shown in bold. The infrared bands in the  $Cu_nCO$  complexes correspond to the elemental Cu, Cu-C and C–O stretching vibrational modes. As the absorption peaks related to the terminal CO appears in the frequency range 2100-1920  $cm^{-1}$  and of elemental Cu and Cu-C stretching mode in 400-200  $cm^{-1}$ , the full range of measured spectra were divided into two parts: 2100-1800  $cm^{-1}$  and 400-200  $cm^{-1}$ . The stretching frequency reduction of terminally-bound CO (in  $Cu_nCO$  complexes)

from the value observed for the gas phase molecule (2143  $cm^{-1}$ ) [26] can be clarified in terms of the Dewar-Chatt [27] or Blyholder model [15] for the bonding of CO to Cu metal nanoclusters. The bond length of a free CO molecule in the gas phase was 1.128 Å [28]. In these complexes, the C–O bond stretches 0.002-0.12 Å with respect to the gas phase, which makes a red-shift in the CO frequency and thus leads to the titled adsorption geometry. When considering the absorption peak intensity, the intensity of the bands increased with the increase of Cu atoms in the cluster. Moreover, it was confirmed that the CO adsorption on Cu nanoclusters was chemisorption in nature with Cu–C bond length (adsorption height) in the range of 1.85-1.92 Å.

The positive adsorption energy for the CO adsorbed on all the  $Cu_n$  nanoclusters measured in this study confirmed the thermodynamic favorability of the adsorption process, with the adsorption energy being maximum (27.9 kcal/mol) for  $Cu_4CO$ .

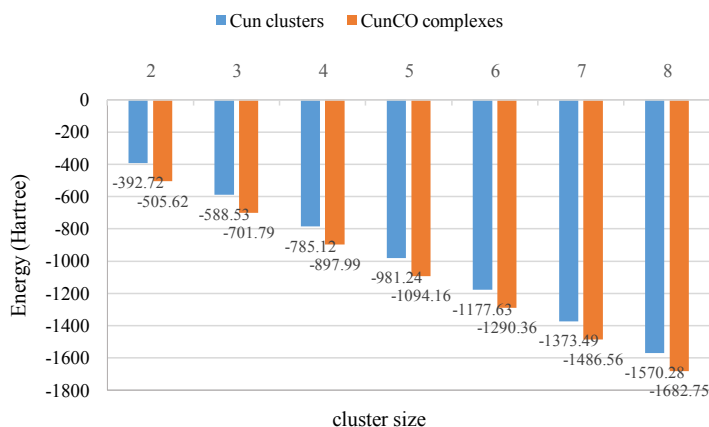


Fig. 2: Energy comparison of  $Cu_n$  nanoclusters and  $Cu_nCO$  complexes.

Table 4. Calculated frequencies for the  $Cu_n$  nanoclusters and  $Cu_nCO$  complexes. The most intense frequencies are shown in bold.

Frequencies ( $cm^{-1}$ )		Frequencies ( $cm^{-1}$ )	
$Cu_2$	258	$Cu_2CO$	212, 218, 238, 250, and 2052 (CO stretching)
$Cu_3$	91, 156, 242	$Cu_3CO$	152, 210, 321, and 1950 (CO stretching)
$Cu_4$	45, 102, 139, 174, 194, 218, 249	$Cu_4CO$	120, 220, 350, 400, and 1999 (CO stretching)
$Cu_5$	46, 98, 127, 169, 196, 215, 250	$Cu_5CO$	25, 50, 170, 250, 340, and 2013 (CO stretching)
$Cu_6$	25, 38, 54, 97, 118, 171, 194, 251, 255	$Cu_6CO$	35, 56, 63, 79, 252, 262, and 1997 (CO stretching)
$Cu_7$	71, 109, 125, 128, 137, 153, 205, 211, 224	$Cu_7CO$	51, 99, 126, 145, 256, and 1982 (CO stretching)
$Cu_8$	69, 75, 102, 121, 163, 178, 216, 220	$Cu_8CO$	56, 69, 230, 271, 350, and 2007 (CO stretching)

To gain an overall view of the electronic structures of  $Cu_nCO$  complexes, the density of states (DOSs) of  $Cu_n$  nanoclusters and  $Cu_nCO$  complexes along with the HOMO and LUMO pictures are shown in Figs. 3-9. These pictures helped us to recognize the areas where electron density was concentrated. The positive and negative phases are represented in red and green

colors, respectively. It was found that the CO molecule specifically adsorb over the high electron density area, *i.e.*, HOMO of  $Cu_n$  nanoclusters. After CO chemisorption, the d-band shifted deeper in energy. Also notable was the nearness of the band of the occupied states to the Fermi level of the metal and to the band of the lowest unoccupied states.

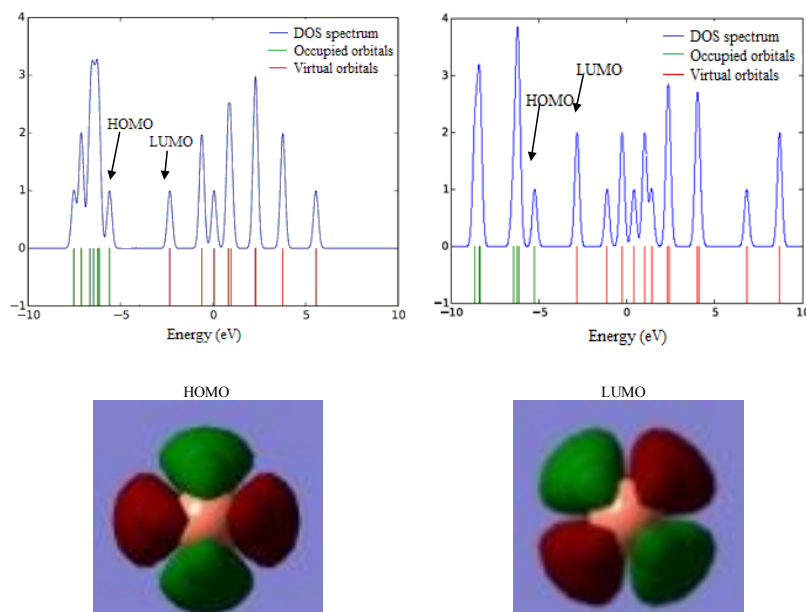


Fig. 3: DOS of  $Cu_2$  nanocluster (Left), DOS, HOMO and LUMO pictures of  $Cu_2CO$  complex (Right).

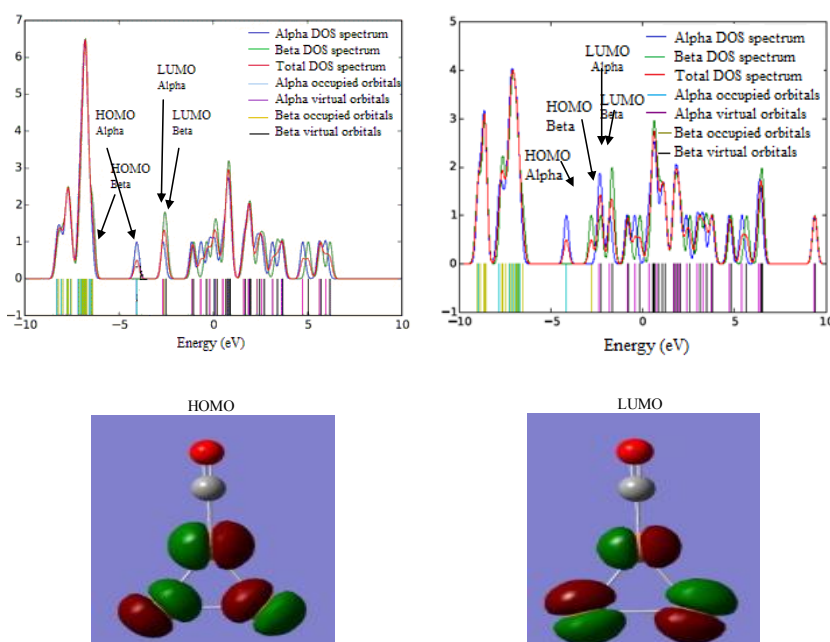


Fig. 4: DOS of  $Cu_3$  nanocluster (Left), DOS, HOMO and LUMO pictures of  $Cu_3CO$  complex (Right).

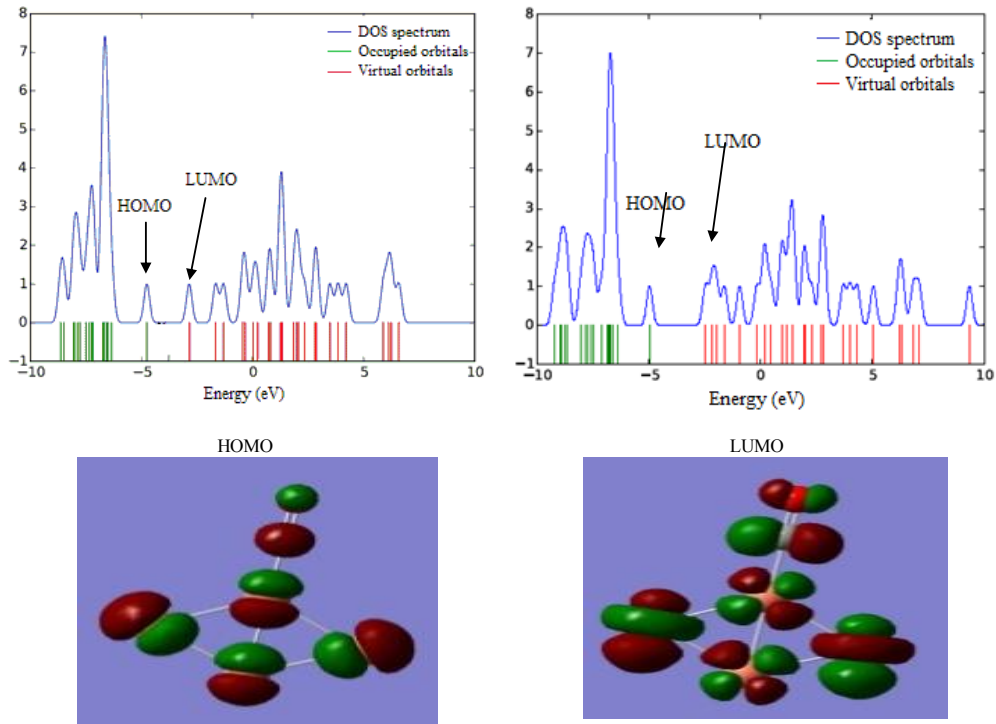


Fig. 5: DOS of  $\text{Cu}_4$  nanocluster (Left), DOS, HOMO and LUMO pictures of  $\text{Cu}_4\text{CO}$  complex (Right).

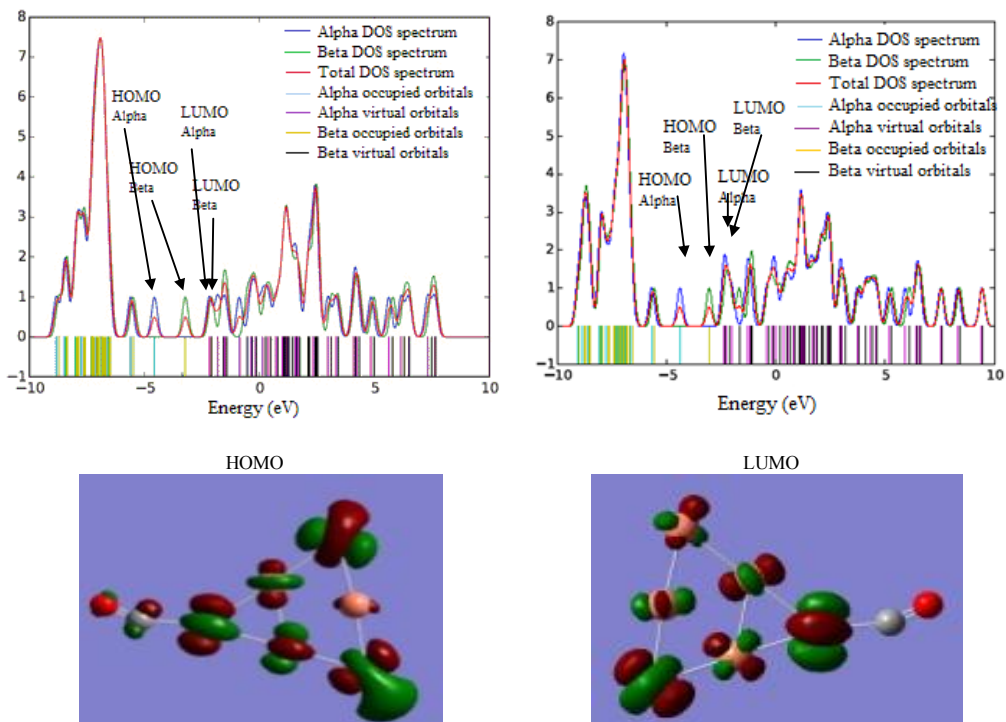


Fig. 6: DOS of  $\text{Cu}_5$  nanocluster (Left), DOS, HOMO and LUMO pictures of  $\text{Cu}_5\text{CO}$  complex (Right).

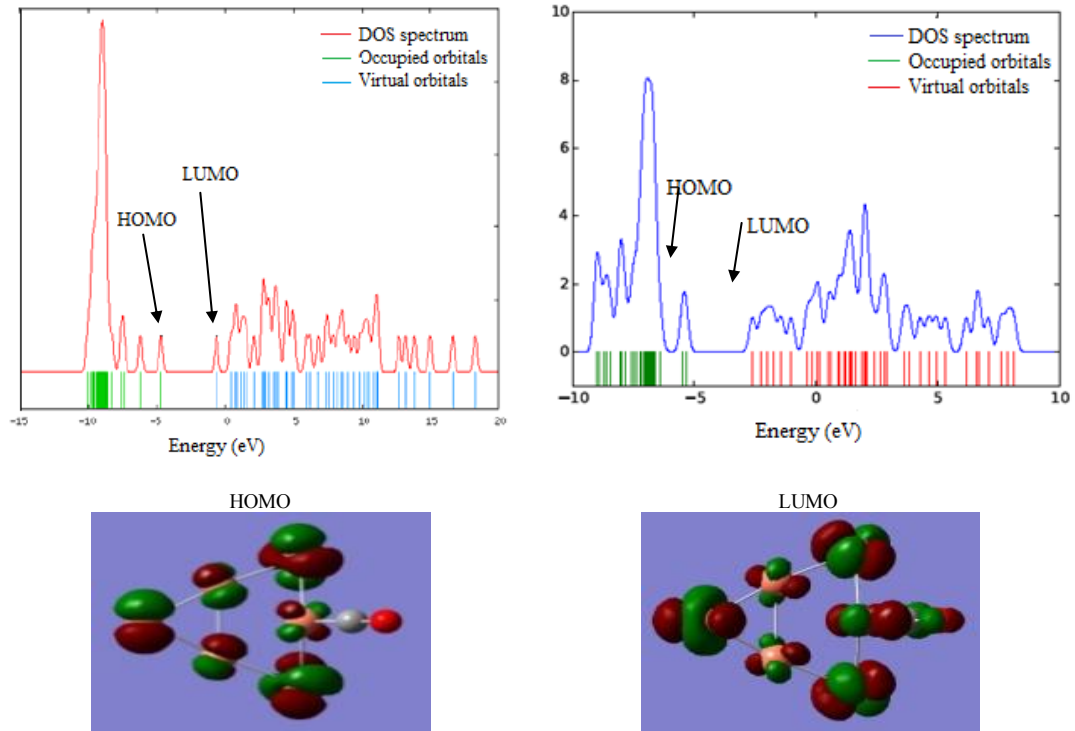


Fig. 7: DOS of  $\text{Cu}_6$  nanocluster (Left), DOS, HOMO and LUMO pictures of  $\text{Cu}_6\text{CO}$  complex (Right).

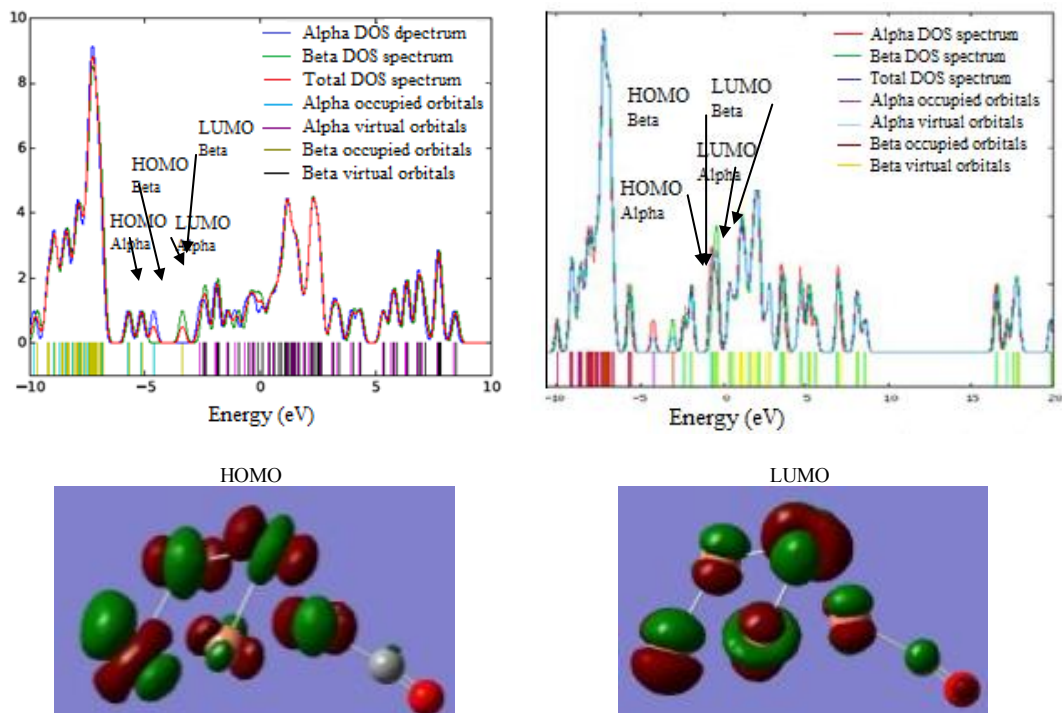


Fig. 8: DOS of  $\text{Cu}_6$  nanocluster (Left), DOS, HOMO and LUMO pictures of  $\text{Cu}_6\text{CO}$  complex (Right).



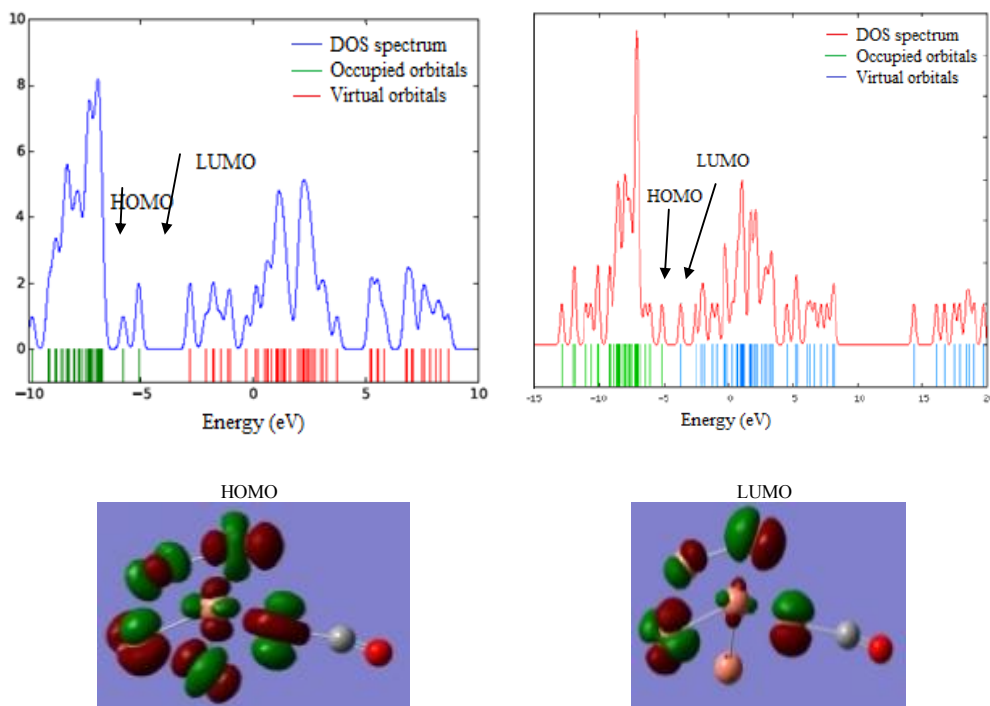


Fig. 9: DOS of  $\text{Cu}_8$  nanocluster (Left), DOS, HOMO and LUMO pictures of  $\text{Cu}_8\text{CO}$  complex (Right).

## CONCLUSIONS

Copper nanoparticles have been identified as an important catalytic agent in supported metal catalysts for CO oxidation. In this paper, first-principle calculations under generalized gradient approximation were carried out to investigate the adsorption of CO over  $\text{Cu}_n$  nanoclusters. The binding energy, dipole moment, vibrational frequency, and IR intensity as well as the HOMO-LUMO energy gap and the electronic density of states (DOS) were obtained. The results showed the CO adsorption energy and C-O vibrational frequency on the  $\text{Cu}_n$  nanoclusters and led to the following conclusions:

- The planar configuration (2D) was the most stable structure among the  $\text{Cu}_n$  nanoclusters.
- The CO adsorbed on  $\text{Cu}_n$  nanoclusters showed a stretch frequency at  $1950\text{--}2052\text{ cm}^{-1}$ , which was red-shifted relative to that of gas-phase CO ( $2143\text{ cm}^{-1}$ ). This red-shift was believed to arise from the charge transfer from the Cu metal d states to the CO antibonding  $2\pi^*$  level.
- The HOMO-LUMO energy gap changed upon CO adsorption.
- The CO molecule specifically adsorbed over the high electron density area, i.e., HOMO of  $\text{Cu}_n$  nanoclusters.

- The CO adsorption on  $\text{Cu}_n$  nanoclusters was chemisorption in nature with the Cu-C bond length (adsorption height) in the range of  $1.85\text{--}1.92\text{ \AA}$ .
- The positive adsorption energy for CO adsorbed on all the  $\text{Cu}_n$  nanoclusters measured in this study confirmed the thermodynamic favorability of the adsorption process.
- The strongest CO adsorption existed in the  $\text{Cu}_4$  nanocluster ( $27.9\text{ kcal/mol}$ ).

## CONFLICT OF INTEREST

The authors declare that there is no conflict of interests regarding the publication of this manuscript.

## REFERENCES

- [1] Haberland H., (1994), *Clusters of Atoms and Molecules*, First ed., Berlin: Springer.
- [2] Braunstein P., Oro L. A., Raithby P. R., (1999), *Metal Clusters in Chemistry*, First ed., Weinheim: Wiley-VCH.
- [3] Rošch N., Pacchioni G., (1994), *Clusters and Colloids: From Theory to Applications*, First ed., Weinheim: Verlag Chemie.
- [4] Xu H. X., Suslick K. S., (2010), Sonochemical synthesis of highly fluorescent Ag nanoclusters. *ACS Nano*. 4: 3209-3212.
- [5] González B. S., Rodríguez M. J., Blanco C., (2010), One step synthesis of the smallest photoluminescent and paramagnetic PVP-protected gold atomic clusters. *Nano Lett.* 10: 4217-4221.
- [6] Guvelioglu G. H., Ma P., He X., Forrey R. C., Cheng H.,

- (2005), Evolution of Small Copper Clusters and Dissociative Chemisorption of Hydrogen. *phys. Rev. Lett.* 94: 0261031-4.
- [7] Chen W., Chen S. W., (2009), Oxygen electroreduction catalyzed by gold nanoclusters: Strong core size effects. *Angew. Chem. Int. Ed.* 48: 4386-4390.
- [8] Huang T. J., Tsai D. H., (2003), CO Oxidation Behavior of Copper and Copper Oxides. *Catal. Lett.* 87: 173-179.
- [9] Muettterties E. L., Rhodin T. N., Band E., Brucker C. F., Pretzer W. R., (1979), Clusters and surfaces. *Chem. Rev.* 79: 91-96.
- [10] Frenking G., Fröhlich N., (2000), The nature of the bonding in transition-metal compounds. *Chem. Rev.* 100: 717-722.
- [11] Zhou M., Andrews L., Bauschlicher C. W., (2001), Spectroscopic and theoretical investigations of vibrational frequencies in binary unsaturated transition-metal carbonyl cations, neutrals, and anions. *Chem. Rev.* 101: 1931-1936.
- [12] Jernigan G. G., Somorjai G. A., (1994), Carbon monoxide oxidation over three different oxidation states of copper: Metallic copper, copper (I) oxide, and copper (II) oxide: A surface science and kinetic study. *J. Catal.* 147: 567-572.
- [13] Pillai R. U., Deevi S., (2006), Room temperature oxidation of carbon monoxide over copper oxide catalyst. *Appl. Catal. B.* 64: 146-152.
- [14] White B., Yin M., Hall A., Le D., Stolbov S., Rahman T., Turro N., O'Brien S., (2006), Complete CO oxidation over Cu<sub>2</sub>O nanoparticles supported on Silica gel. *Nano Lett.* 6: 2095-2099.
- [15] Blyholder G., (1964), Molecular orbital view of chemisorbed carbon monoxide. *J. Chem. Phys.* 68: 2772-2776.
- [16] Burda C., Chen X. B., Narayanan R., El-Sayed M. A., (2005), Chemistry and properties of nanocrystals of different shapes. *Chem. Rev.* 105: 1025-1032.
- [17] Lee C., Yang W., Parr R. G., (1988), Development of the Colle-Salvetti Correlation Energy Formula into a Functional of the Electron Density. *Phys. Rev. B.* 37: 785-789.
- [18] Wadt W. R., Hay P. J., (1985), Ab initio effective core potentials for molecular calculations. Potentials for the transition metal atoms Sc to Hg. *J. Chem. Phys.* 82: 270-275.
- [19] Glockler G., (1958), Carbon-Oxygen Bond Energies and Bond Distances. *J. Phys. Chem.* 62: 1049-1054.
- [20] Frisch M. J., Trucks G. W., Schlegel H. B., Scuseria G. E., Robb M. A., Cheeseman J. R., Scalmani G., Barone V., Mennucci B., Petersson G. A., Nakatsuji H., Caricato M., Li X., Hratchian H. P., Izmaylov A. F., Bloino J., Zheng G., Sonnenberg J. L., Hada M., Ehara M., Toyota K., Fukuda R., Hasegawa J., Ishida M., Nakajima T., Honda Y., Kitao O., Nakai H., Vreven T., Montgomery J. A., Peralta J. E., Ogliaro F., Bearpark M., Heyd J. J., Brothers E., Kudin K. N., Staroverov V. N., Kobayashi R., Normand J., Raghavachari K., Rendell A., Burant J. C., Iyengar S. S., Tomasi J., Cossi M., Rega N., Millam J. M., Klene M., Knox J. E., Cross J. B., Bakken V., Adamo C., Jaramillo J., Gomperts R., Stratmann R. E., Yazyev O., Austin A. J., Cammi R., Pomelli C., Ochterski J. W., Martin R. L., Morokuma K., Zakrzewski V. G., Voth G. A., Salvador P., Dannenberg J. J., Dapprich S., Daniels A. D., Farkas O., Foresman J. B., Ortiz J. V., Cioslowski J., Fox D. J., (2009), *Gaussian 09, Revision A.02*, Gaussian, Inc., Wallingford CT.
- [21] Kahnouji H., Najafvandzadeh H., Hashemifar J., Alaei M., Akbarzadeh H., (2015), Density-functional study of the pure and palladium doped small copper and silver clusters. *Chem Phys Lett.* 630: 101-107.
- [22] Guvelioglu G. H., Ma P., He X., Forrey R. C., Cheng H., (2006), First principles studies on the growth of small Cu clusters and the dissociative chemisorption of H<sub>2</sub>. *phys. Rev. B.* 73: 155436(1-10).
- [23] Huber K. P., Herzberg G., (1979), *Molecular Spectra and Molecular Structure: Constants of Diatomic Molecules*, First ed., New York: Van Nostrand.
- [24] Rohlffing E. A., Valentini J. J., (1986), UV laser excited fluorescence spectroscopy of the jet-cooled copper dimer. *J. Chem. Phys.* 84: 6560-6566.
- [25] Zhan C. G., Nichols J. A., Dixon D. A., (2003), Ionization potential, electron affinity, electronegativity, hardness, and electron excitation energy: Molecular properties from density functional theory orbital energies. *J. Phys. Chem A.* 107: 4184-4188.
- [26] Moudgil H. K., (2010), *Text book of physical chemistry*, First ed., New Delhi: PHI Learning.
- [27] Dewar M. J. S., (1951), A review of  $\pi$  Complex Theory. *Bull. Soc. Chim. Fr.* C71.
- [28] Stépan K., Dürr M., Güdde J., Höfer U., (2005), Laser-induced diffusion of oxygen on a stepped Pt (111) surface. *Surf. Sci.* 593: 54-58.